Light fragment emission in ^{86}Kr-^{124}Sn collisions at 25 MeV/nucleon

Fu-Hu Liu,* Jun-Sheng Li, and Mai-Ying Duan†
Institute of Theoretical Physics, Shanxi University, Taiyuan, Shanxi 030006, People's Republic of China
(Received 27 January 2007; published 21 May 2007)

Light fragments emitted in ^{86}Kr-^{124}Sn collisions at intermediate energy ($E_{\rm beam}$ = 25 MeV/nucleon) and larger impact parameters (b = 7–10 fm) are studied by a multisource ideal gas model. The momentum component, transverse momentum, and azimuthal angle distributions of light fragments with mass numbers A = 1–4 are given. Meanwhile, the correlation between the elliptic flow and transverse momentum, as well as the correlation between the fourth momentum anisotropy and transverse momentum for the mentioned light fragments are given, too. The calculated results are compared with the theoretical results of the Isospin-Dependent Quantum Molecular Dynamics model.

DOI: 10.1103/PhysRevC.75.054613 PACS number(s): 24.75.+i, 25.85.Ge, 21.10.Tg

I. INTRODUCTION

Heavy ion collisions at intermediate and high energies are interesting subjects in theoretical and experimental nuclear physics because these collisions provide a unique opportunity to investigate the particle productions, interacting mechanisms, and rare phenomena at high density and high temperature [1–7]. In particular, a few decades MeV/nucleon is considered to be the low stage of intermediate energy. In the low-energy region (a few MeV/nucleon and below) and high-energy region (a few GeV/nucleon and above), the particle productions and interacting mechanisms are respectively expected to be different.

Many experimental results of heavy ion collisions at intermediate and high energies were reported in the past decades [8–12]. Meanwhile, more theoretical models have been suggested to explain the experimental results [13–17]. To describe the fragments emission process, we have suggested a multisource ideal gas (MSIG) model and explained the azimuthal and polar angle distributions of fragments produced in the projectile and target nuclei over an energy range from the AGS (2–15 GeV/nucleon) to SPS (20–200 GeV/nucleon) by the Monte Carlo method [18–21]. It is interesting for us to test the MSIG model at intermediate energy.

Recently, Yan *et al.* [22] studied light fragments emission in ^{86}Kr-^{124}Sn collisions at intermediate energy ($E_{\rm beam}$ = 25 MeV/nucleon) and larger impact parameters (b = 7–10 fm) by the Isospin-Dependent Quantum Molecular Dynamics (IDQMD) model. The results related to the momentum component, transverse momentum, azimuthal angle, elliptic flow, and fourth momentum anisotropy of the light fragments with mass numbers A = 1–4 are given [22]. To test the MSIG model at the intermediate energy region, in this paper, we use it to describe the calculated results of the IDQMD model.

II. MSIG MODEL AND FORMULATION

The IDQMD model can be found in Ref. [22] and references therein. The MSIG model can be found in our previous work [18–21]. To give a whole presentation of the present work, we describe the MSIG model shortly in the following. Let the impact parameter axis be the ox axis and the beam direction be the oz axis. The xoz plane is naturally the reaction plane. Many emission sources of fragments (or particles) are assumed to be formed in spectator (or participant) in high energy heavy ion collisions. At intermediate energy, we assume that many emission sources of fragments are formed in the interacting system. Each emission source is treated as an ideal gas source. The electromagnetic interactions among different emission sources and the asymmetry of mechanics between the projectile and target nuclei affect the emission of fragments (or particles).

In the rest frame of the emission source, the three components p'_x, p'_y, and p'_z of the momentum p' of the final-state fragments are assumed to obey Gaussian distributions with the same standard deviation σ. Considering the interactions among different emission sources and the mechanics asymmetry, the concerned source will have expansions and movements in the momentum space. The simplest relation between the momentum p' in the source rest frame and the momentum p in the final state is linear at nonrelativistic energy. We have

$$p_{x,y,z} = a_{x,y,z}p'_{x,y,z} + B_{x,y,z} = a_{x,y,z}p'_{x,y,z} + b_{x,y,z}\sigma, \quad (1)$$

where $B_{x,y,z}$ represents the movements of the emission source, and $a_{x,y,z}$ and $b_{x,y,z}$ are coefficients describing the expansions and movements of the source, respectively.

In the case of considering physics quantities in the transverse plane, the z component does not need to be included. According to probability theory and Eq. (1), the distribution of $p_{x,y}$ can be given by

$$f_{p_{x,y}}(p_{x,y}) = \frac{1}{\sqrt{2\pi}\sigma a_{x,y}} \exp\left[-\frac{(p_{x,y} - b_{x,y}\sigma)^2}{2\sigma^2 a_{x,y}^2} \right]. \quad (2)$$

*Electronic address: fuhuliu@163.com
†Electronic address: duanmaiying@163.com

The united density function of p_x and p_y is

$$f_{p_x,p_y}(p_x, p_y) = f_{p_x}(p_x) f_{p_y}(p_y) = \frac{1}{2\pi\sigma^2 a_x a_y} \times \exp\left[-\frac{(p_x - b_x\sigma)^2}{2\sigma^2 a_x^2} - \frac{(p_y - b_y\sigma)^2}{2\sigma^2 a_y^2} \right]. \quad (3)$$

Considering the transverse momentum

$$p_T \equiv \sqrt{p_x^2 + p_y^2} \quad (4)$$

and the azimuthal angle

$$\varphi \equiv \arctan \frac{p_y}{p_x}, \quad (5)$$

we have for the united density function of p_T and φ

$$f_{p_T,\varphi}(p_T, \varphi) = p_T f_{p_x,p_y}(p_T \cos\varphi, p_T \sin\varphi) = \frac{p_T}{2\pi\sigma^2 a_x a_y} \exp\left[-\frac{(p_T\cos\varphi - b_x\sigma)^2}{2\sigma^2 a_x^2} - \frac{(p_T \sin\varphi - b_y\sigma)^2}{2\sigma^2 a_y^2} \right]. \quad (6)$$

Thus, the p_T distribution is

$$f_{p_T}(p_T) = \int_0^{2\pi} f_{p_T,\varphi}(p_T, \varphi)\mathrm{d}\varphi, \quad (7)$$

and the φ distribution is

$$f_\varphi(\varphi) = \int_0^{\max} f_{p_T,\varphi}(p_T, \varphi)\mathrm{d}p_T. \quad (8)$$

The n-th momentum anisotropy can be given by

$$v_n \equiv \langle\cos(n\varphi)\rangle = \int_0^{2\pi} \cos(n\varphi) f_\varphi(\varphi)\mathrm{d}\varphi = \int_0^{2\pi} \cos(n\varphi) \int_0^{\max} f_{p_T,\varphi}(p_T, \varphi)\mathrm{d}p_T\mathrm{d}\varphi. \quad (9)$$

In the Monte Carlo calculation, let R_1, R_2, R_3, R_4, R_5, and R_6 denote random variables distributed in [0,1]. We have

$$p'_{x,y} = \sqrt{-2\ln R_{1,3}}\cos(2\pi R_{2,4})\sigma \quad (10)$$

because $p'_{x,y}$ obeys the Gaussian distribution. Considering Eqs. (1), (4), and (5), the momentum component, transverse momentum, and azimuthal angle can be written as

$$p_{x,y} = \sigma[a_{x,y}\sqrt{-2\ln R_{1,3}}\cos(2\pi R_{2,4}) + b_{x,y}], \quad (11)$$

$$p_T = \sigma\sqrt{\left[a_x\sqrt{-2\ln R_1}\cos(2\pi R_2) + b_x\right]^2 + \left[a_y\sqrt{-2\ln R_3}\cos(2\pi R_4) + b_y\right]^2}, \quad (12)$$

and

$$\varphi = \arctan\frac{a_y\sqrt{-2\ln R_3}\cos(2\pi R_4) + b_y}{a_x\sqrt{-2\ln R_1}\cos(2\pi R_2) + b_x}, \quad (13)$$

respectively. The elliptic flow (the second momentum anisotropy) is

$$v_2 \equiv \langle\cos(2\varphi)\rangle = \left\langle\frac{p_x^2 - p_y^2}{p_T^2}\right\rangle \quad (14)$$

and the fourth momentum anisotropy is

$$v_4 \equiv \langle\cos(4\varphi)\rangle = \left\langle\frac{p_x^4 - 6p_x^2p_y^2 + p_y^4}{p_T^4}\right\rangle. \quad (15)$$

From the above discussions, we see that two methods can be used to calculate the distributions of momentum components, transverse momentum, and azimuthal angle. On the correlations between v_2 and p_T, as well as v_4 and p_T, the Monte Carlo method is more convenient. For the purpose of convenience, in this paper we use the Monte Carlo method to calculate the concerned physics quantities. The related distributions and correlations can be obtained by a statistical method. An isotropic emission in the transverse plane gives $a_{x,y} = 1$ and $b_{x,y} = 0$. The physics condition gives $a_{x,y} \geqslant 1$. The number and excitation degrees of emission sources do not affect the azimuthal angle. Because the parameters $b_{x,y}$ are normalized to the width of the momentum distribution, the expression for φ does not contain the parameter σ. This allows us to describe the particle angular distribution in a way that is independent of the source temperature. The parameters $B_{x,y}$ describe how much the source is displaced from the beam axis or what the average transverse momentum of the source is, and the parameters $b_{x,y}$ describe only the displacement coefficient of the source.

III. COMPARISON WITH CALCULATED RESULTS OF IDQMD MODEL

The p_x/A distributions, $A\mathrm{d}N/\mathrm{d}p_x$, for the light fragments with $A = 1$–4 produced in ^{86}Kr-^{124}Sn collisions at 25 MeV/nucleon and larger impact parameters (7–10 fm) are given in Fig. 1. The circles are the calculated results of the IDQMD model quoted in Ref. [22]. The solid curves are our calculated results by the MSIG model. For the protons (Fig. 1(a)), we take $a_x = 1.16$, $b_x = -0.05$, and $\sigma = 0.098$ GeV/c; for $A = 2$ (Fig. 1(b)), we take $a_x = 1.30$, $b_x = -0.18$, and $\sigma = 0.128$ GeV/c; for $A = 3$ (Fig. 1(c)), we take $a_x = 1.48$, $b_x = -0.10$, and $\sigma = 0.159$ GeV/c; and for $A = 4$ (Fig. 1(d)), we take $a_x = 1.70$, $b_x = -0.15$, and $\sigma = 0.180$ GeV/c. For $A = 1$–4, the values of a_y and b_y are taken to be 1 and 0, respectively. In the selection of the parameter

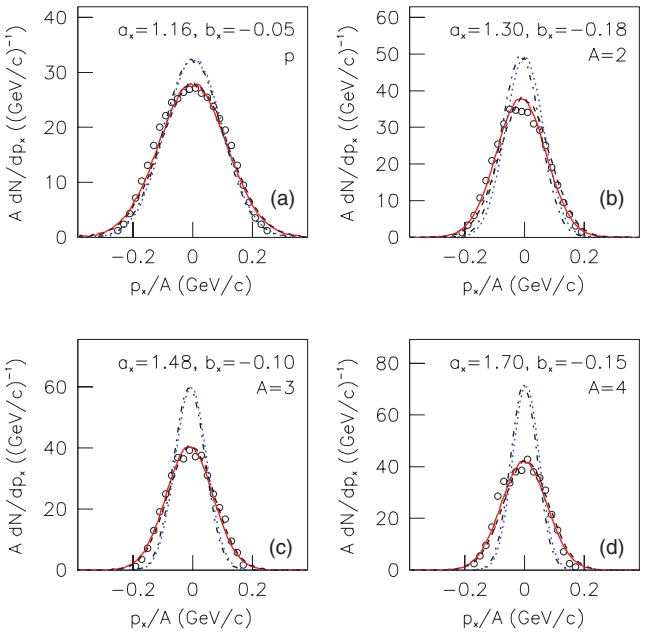

FIG. 1. (Color online) The p_x/A distributions, $A\mathrm{d}N/\mathrm{d}p_x$, for the light fragments with $A = 1$–4 produced in ^{86}Kr-^{124}Sn collisions at 25 MeV/nucleon and larger impact parameters (7–10 fm). The circles are the calculated results of the IDQMD model quoted in Ref. [22]. The solid curves are our calculated results by the MSIG model. The other curves are also our calculated results by the MSIG model for the purpose of comparison.

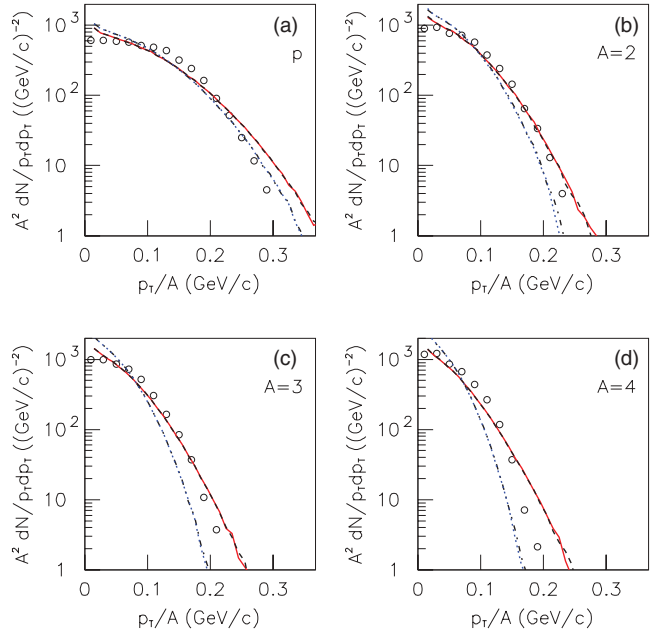

FIG. 2. (Color online) As for Fig. 1, but showing the p_T/A distributions, $A^2\mathrm{d}N/p_T\mathrm{d}p_T$.

values, the method of χ^2-testing is used. From the figure, we see that our calculated results by using the MSIG model are in good agreement with those of the IDQMD model [22]. From the parameter values, we see that the emission source has an expansion along the positive and negative x directions and a movement along the negative x direction. The parameters $a_y = 1$ and $b_y = 0$ mean that the emission source has no expansion and movement along the y direction. To see the different contributions, the calculated results of the MSIG model with $(a_x = 1, b_x = 0)$, [$a_x \neq 1$ (i.e. $a_x = 1.16$, 1.30, 1.48, and 1.70, respectively, for $A = 1$–4), $b_x = 0$], and [$a_x = 1$, $b_x \neq 0$ (i.e. $b_x = -0.05$, -0.18, -0.10, and -0.15, respectively)] are given in the figure by the dotted, dashed, and dotted-dashed curves, respectively. We see that a_x has a main contribution and b_x has a negligible contribution. In the calculation of the MSIG model, the simulated fragment number for each curve is 5×10^5.

Figures 2 and 3 show the p_T/A distributions $A^2\mathrm{d}N/p_T\mathrm{d}p_T$ and the φ distributions $k\mathrm{d}N/\mathrm{d}\varphi$, respectively, for the light fragments with $A = 1$–4 produced in ^{86}Kr-^{124}Sn collisions at 25 MeV/nucleon and larger impact parameters (7–10 fm). The circles are the calculated results of the IDQMD model quoted in Ref. [22]. The solid curves are our calculated results by the MSIG model. The factor k is chosen in the label of longitudinal axis in Fig. 3 so that the mean values of $k\mathrm{d}N/\mathrm{d}\varphi$ are fixed to be 1 [22]. In the calculation, the parameter values are taken as the same as those for Fig. 1. We see that the two kinds of calculated results for the p_T/A distributions are qualitatively in agreement with each other. For the φ distributions the two calculations are in good agreement with each other, and the contributions of b_x are obvious. For comparison, the dotted, dashed, and dotted-dashed curves in Figs. 2 and 3 represent our calculated results with $(a_x = 1, b_x = 0)$, $(a_x \neq 1, b_x = 0)$, and $(a_x = 1, b_x \neq 0)$, respectively. In the calculation of the MSIG model, the simulated fragment number for each curve is 5×10^5.

The dependences of v_2/A on p_T/A and v_4/A on p_T/A for the light fragments with $A = 1$–4 produced in ^{86}Kr-^{124}Sn collisions at 25 MeV/nucleon and larger impact parameters

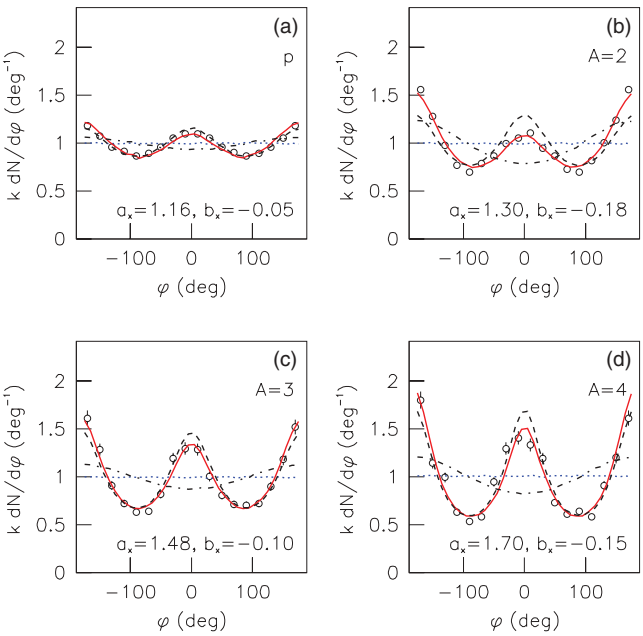

FIG. 3. (Color online) As for Fig. 1, but showing the φ distributions, $k\mathrm{d}N/\mathrm{d}\varphi$.

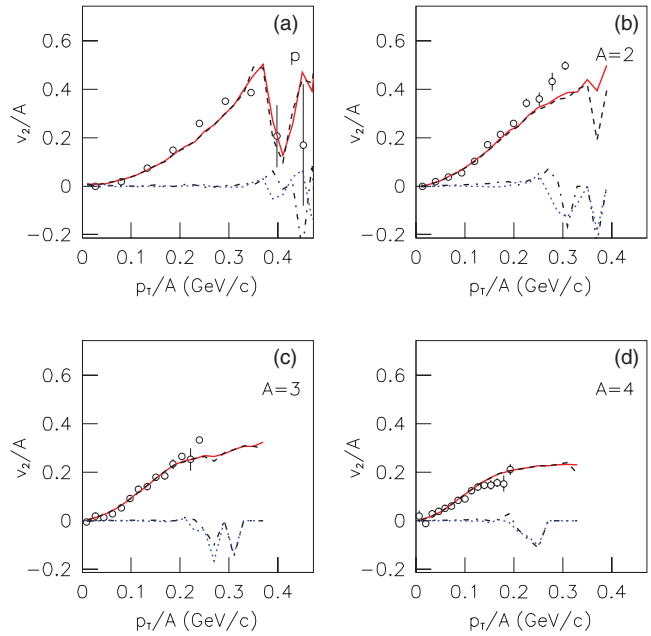

FIG. 4. (Color online) The correlations between v_2/A and p_T/A for the light fragments with $A = 1$–4 produced in ^{86}Kr-^{124}Sn collisions at 25 MeV/nucleon and larger impact parameters (7–10 fm). The circles are the calculated results of the IDQMD model quoted in Ref. [22]. The solid curves are our calculated results by the MSIG model. The other curves are also our calculated results by the MSIG model for the purpose of comparison.

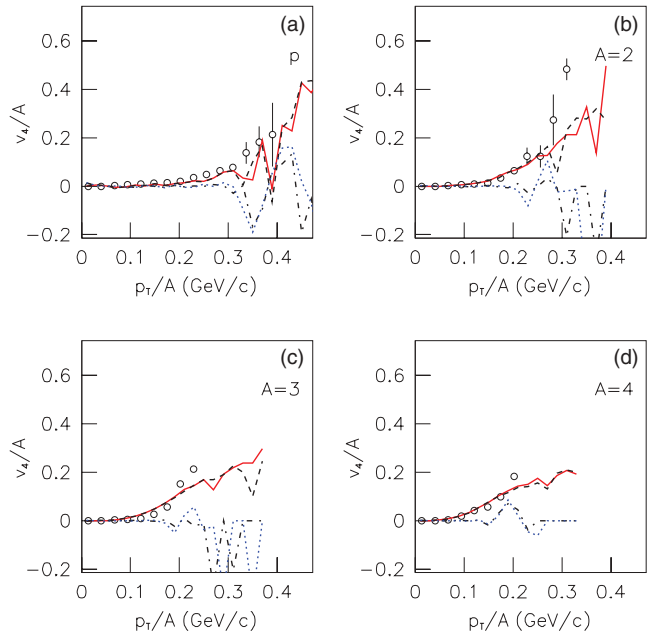

FIG. 5. (Color online) As for Fig. 4, but showing the correlations between v_4/A and p_T/A.

(7–10 fm) are shown in Figs. 4 and 5, respectively. The circles are the calculated results of the IDQMD model quoted in Ref. [22], and the solid curves are our calculated results by the MSIG model. In the calculation, the parameter values are taken as the same as those for Fig. 1. One can see that the two kinds of calculations are approximately in agreement with each other in the case of excluding the results in the high p_T region due to the low statistics. For comparison, the dotted, dashed, and dotted-dashed curves in the figures are our calculated results with $(a_x = 1, b_x = 0)$, $(a_x \neq 1, b_x = 0)$, and $(a_x = 1, b_x \neq 0)$, respectively. In the calculation of the MSIG model, the simulated fragment number for each curve is 5×10^5.

In the above discussion, the parameters $a_{x,y}$ and $b_{x,y}$ reflect the transverse structure of the emission source in the momentum space. The condition $a_x(a_y) > 1$ means that the emission source has expansions along $x(y)$ direction. The condition $b_x(b_y) > 0$ [or $b_x(b_y) < 0$] means that the emission source has movements along the positive $x(y)$ [or negative $x(y)$] direction. An isotropic emission source gives $a_{x,y} = 1$ and $b_{x,y} = 0$. To see the transverse structure of the emission source, Fig. 6 shows the p_y vs. p_x for the light fragments with $A = 1$–4 produced in ^{86}Kr-^{124}Sn collisions at 25 MeV/nucleon and larger impact parameters (7–10 fm). The solid curve circles represent the sources in the p_y-p_x plane and the small full circles are their centers. The dotted curve circles are the original emission sources in the p_y-p_x plane and the small open circles are their centers. Corresponding to the dotted curve circles in Fig. 6, the p_x/A, p_T/A, and φ distributions, as well as the v_2/A-p_T/A and v_4/A-p_T/A correlations, are represented by the dotted curves in Figs. 1–5, respectively. One can see an expansion of the source along the positive and negative x directions and a movement of the source along the negative x direction.

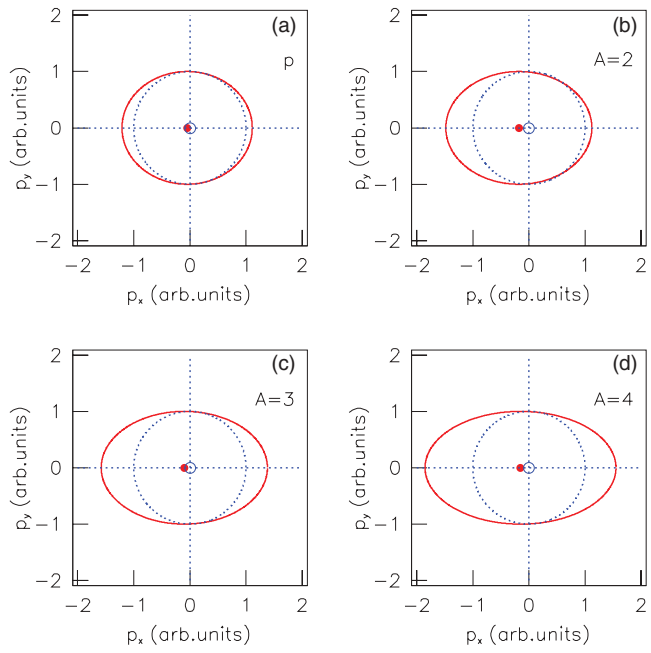

FIG. 6. (Color online) The transverse structure of emission source in the p_y-p_x plane for the light fragments with $A = 1$–4 produced in ^{86}Kr-^{124}Sn collisions at 25 MeV/nucleon and larger impact parameters (7–10 fm). The solid curve circles represent the sources in the p_y-p_x plane and the small full circles are their centers. The dotted curve circles are the original emission sources in the p_y-p_x plane and the small open circles are their centers.

IV. DISCUSSION AND CONCLUSION

The emission of fragments is affected by the electromagnetic interactions among different emission sources and the asymmetry of mechanics between the projectile and target nuclei. These effects cause the emission source to be deformed. Because the *xoz* plane is taken to be the reaction plane, and the *ox* axis is taken to be the impact parameter axis, we should have $a_y = 1$ and/or $b_y = 0$ due to the symmetry of the interacting system and the symmetry of the mechanics around the reaction plane. In the case of existing systematic errors in the measurement of the reaction plane, one expects to have $a_y > 1$ and $b_y \neq 0$. In the transverse plane, the vectors $(a_x - 1)\mathbf{i}+(a_y - 1)\mathbf{j}$ and $b_x\mathbf{i}+b_y\mathbf{j}$ should be at the direction of the impact parameter.

The parameter a_x increases systematically with the light fragment mass. This is caused by the asymmetry of the mechanics. The effect of the mechanics asymmetry is expected to enlarge with increasing fragment mass. The parameter σ increases with the light fragment mass, too. This is caused by the fragment mass itself. According to $\sigma = \sqrt{mT}$, where m and T denote the fragment mass and source temperature respectively, and the values of σ for the light fragments with $A = 1$–4, we have $T = 10.2$, 8.7, 9.0, and 8.6 MeV, respectively. One can see that the source temperatures for the light fragments with $A = 1$–4 are approximately equal to each other.

To conclude, the light fragments produced in heavy ion collisions at intermediate energy and large impact parameter have been studied by using the multisource ideal gas model. Our previous work [18–21] showed that this model is successful over an energy range from a few GeV/nucleon to 200 GeV/nucleon. The distributions of momentum components, transverse momentum, and azimuthal angle, the correlation between the elliptic flow (the second momentum anisotropy) and transverse momentum, as well as the correlation between the fourth momentum anisotropy and transverse momentum for light fragments with the mass numbers 1–4 in ^{86}Kr-^{124}Sn collisions at 25 MeV/nucleon and larger impact parameters (7–10 fm) have been obtained by us. The calculated results are compared with the theoretical results of the Isospin-Dependent Quantum Molecular Dynamics model. It is found that the two kinds of calculated results on the distributions of momentum component and azimuthal angle are respectively in good agreement with each other. On the transverse momentum distribution, the two kinds of calculated results are qualitatively in agreement with each other. For the correlation between the elliptic flow and transverse momentum, as well as for the correlation between the fourth momentum anisotropy and transverse momentum, the two kinds of calculations are approximately in agreement with each other in the case of excluding the calculated results in the high transverse momentum region due to the low statistics.

In the multisource ideal gas model, there are three kinds of parameters: the expansion coefficient $a_x(a_y, a_z)$, the movement coefficient $b_x(b_y, b_z)$, and the excitation degree σ of the source. An expansion effect along $x(y, z)$ direction gives $a_x(a_y, a_z) > 1$, and a movement effect along positive (or negative) $x(y, z)$ direction gives $b_x(b_y, b_z) > 0$ (or < 0). In the case of isotropic emission, the source has no expansion and movement, and we have $a_x(a_y, a_z) = 1$ and $b_x(b_y, b_z) = 0$.

ACKNOWLEDGMENTS

This work was supported by the China Scholarship Council, the National Natural Science Foundation of China Grant Nos. 10675077 and 10275042, the Shanxi Provincial Foundation for Returned Overseas Scholars Grant No. JLGB(2001)15, and the Shanxi Provincial Natural Science Foundation Grant No. 2007011005.

[1] K. Werner, Phys. Rep. **232**, 87 (1993).
[2] M. Murray, J. Phys. G **31**, S1137 (2005).
[3] B. B. Back *et al.* (E917 Collaboration), Phys. Rev. Lett. **86**, 1970 (2001).
[4] B. B. Back *et al.* (E917 Collaboration), Phys. Rev. C **66**, 054901 (2002).
[5] I. G. Bearden *et al.* (BRAHMS Collaboration), Phys. Lett. **B523**, 227 (2001).
[6] I. G. Bearden *et al.* (BRAHMS Collaboration), Phys. Rev. Lett. **88**, 202301 (2002).
[7] B. B. Back *et al.* (PHOBOS Collaboration), Phys. Rev. Lett. **87**, 102303 (2001).
[8] R. Stanoeva, V. Bradnova, P. I. Zarubin, I. G. Zarubina, N. A. Kachalova, A. D. Kovalenko, A. I. Malakhov, P. A. Rukoyatkin, V. V. Rusakova, S. Vokál, G. I. Orlova, N. G. Peresadko, S. P. Kharlamov, E. Stan, M. Haiduc, and I. Tsakov, Talk given at the Conference on Physics of Fundamental Interactions, Moscow, Russia, 5–9 December 2005, nucl-ex/0605013.
[9] B. Hong *et al.* (FOPI Collaboration), Phys. Rev. C **71**, 034902 (2005).
[10] M. El-Nadi, N. Ali-Mossa, and A. Abdelsalam, Nuovo Cimento A **110**, 1255 (1997).
[11] D. Kudzia, B. Wilczyńska, and H. Wilczyński, Phys. Rev. C **68**, 054903 (2003).
[12] G. Singh, K. Sengupta, and P. L. Jain, Phys. Rev. C **41**, 999 (1990).
[13] X. N. Wang and M. Gyulassy, Phys. Rev. Lett. **68**, 1480 (1992).
[14] S. H. Kahana, T. J. Schlagel, and Y. Pang, Nucl. Phys. **A566**, 465c (1994).
[15] Z. W. Lin, S. Pal, C. M. Ko, B. A. Li, and B. Zhang, Nucl. Phys. **A698**, 375 (2002).
[16] H. M. Hofmann and G. M. Hale, Nucl. Phys. **A613**, 69 (1997).
[17] U. Ornik, R. M. Weiner, and G. Wilk, Nucl. Phys. **A566**, 469c (1994).
[18] F. H. Liu, Europhys. Lett. **63**, 193 (2003).
[19] F. H. Liu, N. N. Abd Allah, D. H. Zhang, and M. Y. Duan, Int. J. Mod. Phys. E **12**, 713 (2003).
[20] F. H. Liu, N. N. Abd Allah, and B. K. Singh, Phys. Rev. C **69**, 057601 (2004).
[21] F. H. Liu, Can. J. Phys. **82**, 109 (2004).
[22] T. Z. Yan, Y. G. Ma, X. Z. Cai, J. G. Chen, D. Q. Fang, W. Guo, C. W. Ma, E. J. Ma, W. Q. Shen, W. D. Tian, and K. Wang, Phys. Lett. **B638**, 50 (2006).